PROCEEDINGS OF ECOS 2023 - THE 36TH INTERNATIONAL CONFERENCE ON
EFFICIENCY, COST, OPTIMIZATION, SIMULATION AND ENVIRONMENTAL IMPACT OF ENERGY SYSTEMS
25-30 JUNE, 2023, LAS PALMAS DE GRAN CANARIA, SPAIN

Impact of Detailed Hydropower Representation in National Energy System Modelling

M. Catania[a], F. Parolin[b], F. Fattori[c] and P. Colbertaldo[d]

[a] Department of Energy, Politecnico di Milano, Milan, Italy, matteo.catania@polimi.it, CA
[b] Department of Energy, Politecnico di Milano, Milan, Italy, federico.parolin@polimi.it
[c] Dipartimento di Scienze Teoriche e Applicate, Università degli Studi dell'Insubria, Varese, Italy, fabrizio.fattori@uninsubria.it
[d] Department of Energy, Politecnico di Milano, Milan, Italy, paolo.colbertaldo@polimi.it

Abstract:

Renewables are becoming more and more important due to the ambitious decarbonization targets. In this scenario, the improved integration of hydropower can play a crucial role thanks to its programmable operation, which is a valuable feature. In some countries it is a primary alternative to fossil resources, for example Italy, where hydro currently covers roughly half of the renewable power generation. Hydropower flexibility poses considerable modelling challenges due to the scarce availability of data. This work aims at addressing this research gap, by analysing the impact of hydropower details on energy system models. Using open-source information, a detailed dataset of Italian hydroelectric programmable plants (pumped hydro and reservoirs) is created. For each plant, storage capacity, geographical location, and nominal power are available. The multi-annual historical operational data are exploited to derive a precipitation inflow timeseries for each electricity market bidding zone, which is then distributed on power plants aggregated by administrative region. This new set of data is applied to a multi-node, multi-sector, and multi-vector energy system model, which optimises the design and operation of a carbon-neutral Italian energy system, looking at a 2050 framework with assigned energy vectors demand. Results are compared to those of a fixed-hydropower operation case, thus being able to assess how the modelled flexibility impacts the optimal solution. The analysis favours an improved understanding of future energy systems, helping to shape properly integrated systems with a great amount of non-programmable sources.

Keywords:

Hydropower; Energy dispatch; Integration; Energy system modelling.

1. Introduction

The focus on decarbonization has been increasing steadily over the years, permeating every aspect of society. Within the energy sector, this trend has spurred the growing importance of renewable energy sources (RES), stimulated by ever-more ambitious targets. This demanding path is pushing each technology to find new ways to improve efficiency and economic viability. The European Union has exemplified this trend through initiatives such as FitFor55 [1] and REPowerEU [2], which provide substantial public funds to improve investments and enhance the energy security of the region.

Such initiatives offer an exceptional opportunity for EU countries to gain greater control over their energy supply, thus enhancing their economic stability and security. This could help to mitigate the impact of global energy market fluctuations, which is particularly important for countries with high dependence on imported energy sources. For instance, Italy suffered significant economic consequences in 2022 as a result of its heavy reliance on gas and oil imports. Renewable energy sources, on the other hand, offer countries the necessary autonomy. This is particularly true when the manufacturing of RES-based technologies is not reliant on critical materials, which may otherwise hinder the achievement of climate targets.

Within this framework, hydroelectric power generation is a crucial asset, since it is a clean energy source that does not require the use of rare or strategical elements for its construction. In addition, unlike solar and wind sources, its operations can be programmed to fit the needs of the grid. Accordingly, its smart integration can lead to an important reduction of CO_2 emissions and to a better design of the energy system reducing the duty of other storage options.

Even if the flexibility of hydropower is relevant for realistic analyses, its accurate integration in Energy System Models (ESMs) is often challenging. This can be attributed to the absence of a unified dataset that lists all

https://doi.org/10.52202/069564-0177

hydroelectric plants and their corresponding rated power and storage capacity. Hydropower modelling in ESMs typically relies on the Joint Research Center (JRC) database [3], which provides data on hydroelectric power generation at a plant-specific level and is continuously updated over the years. However, numerous plants are not included in the database, and energy capacity data of reservoir systems are often unavailable. Looking at a country or continental scale, the available hydroelectric power and energy capacities result considerably underestimated. This data deficiency is common also to Italy, and it is also compounded by the difficulty in obtaining precipitation inflow profiles for each hydroelectric plant. As a result, aggregated data are often utilized, leading to higher levels of uncertainty in the results.

This work aims at addressing this research gap, by analysing the impact of hydropower flexibility on carbon-neutral integrated energy systems, focusing on the case of Italy. Using open-source information, a detailed dataset of Italian hydroelectric programmable plants (pumped hydro and reservoirs) is developed. This provides the storage capacity, geographical location, and nominal power of each plant, as well as the inflow time series by region (NUTS-2 areas). Such database is exploited to investigate the impact of hydropower operation in the Italian energy system using OMNI-ES, a multi-node, multi-sector, and multi-vector ESM, which optimizes the total annual cost, under the constraint of net-zero CO_2 emissions for a target year with assigned demand of energy vectors. To conclude, results are compared to a case with fixed hydropower operation based on historical hydroelectric power generation profiles. The structure of this work is the following: Section 2 describes the methodology developed for the gathering and elaboration of the required data. The model used is presented in Section 3, where also the scenario description and the assumption for the simulation are presented. The main results are then shown and discussed in Section 3, and finally, the key conclusions are summed up in Section 4.

2. Methods and data

This section introduces the methodological approach of the analysis. This includes the development of the Italian hydropower database (Section 2.1), the description of the OMNI-ES model (Section 2.2), the design of the assessed scenario (Section 2.3), and the modelling of hydroelectric plants (Section 2.4).

2.1. Hydro power generation and storage data in Italy

Hydroelectric power plants can be divided into three main technologies: run-of-river (RoR), hydro water reservoir (HWR), and pumped hydro storage (PHS). The first takes water from the flow of the rivers to generate electricity, thus representing a non-programmable source. HWR plants, instead, use dams to create basins that enable long-term energy storage. PHS is analogous, but it offers the possibility to pump water back to the upstream basin, allowing for cyclic operation. Accordingly, HWR and PHS guarantee dispatchable electricity, and their operation can be optimised according to the need of the grid.

To investigate the role of HWR and PHS in decarbonised scenarios, this work develops a detailed database of the existing plants in Italy. Hydroelectric power generation has historically been a relevant source of energy in Italy due to the country's favourable natural conditions. However, the construction of dams in almost all the suitable locations has already taken place, leaving limited scope for new installations. Consequently, hydroelectricity is expected to have lower relevance in the Italian energy system in future scenarios compared to solar photovoltaic and onshore wind [4], which feature a significantly larger potential of capacity expansion [5]. Although hydroelectric power generation faces limited opportunities for expansion, it could still provide a crucial contribution to the energy system, offering the opportunity to perform long-term storage (from weekly and monthly to seasonal) avoiding investments for new installations and reducing the risk of curtailment of solar and wind electricity. The existing databases of the national transmission system operator (TSO) [6] and ENTSO-E [7] are characterised by a poor spatial resolution, as data are aggregated either at national or bidding zone level. However, recent studies have shown that in systems where renewables dominate, grid dispatchability cannot be guaranteed, thus requiring a higher level of spatial resolution to incorporate possible congestion limits [5,8]. In addition, the available open-source databases lack information on the energy storage capacity of HWR and PHS plants. To fill these gaps, this works develops a comprehensive dataset of Italian HWR and PHS systems, providing the energy capacity and location of each plant.

The analysis starts from the JRC hydropower database [3], which provides reliable data for what concerns the plants name and power capacity. However, only few of them feature the information about the energy capacity, and the comparison with the number of plants provided by the Italian TSO *Terna SpA* [6] shows that a significant number of plants is absent in the JRC database. Specifically, the TSO reports a total of over 4000 plants, whereas the JRC database lists approximately 300 plants. As a result, the JRC database underestimates the national power capacity of hydro by over 20% (19.4 GW_e compared to 24.7 GW_e). Accordingly, a dedicated and detailed search has been carried out to complete the list of plants and to retrieve the energy capacity. The analysis relies on freely accessible sources, largely derived from the websites of plant owners and of the Italian Ministry of infrastructures and transport [9]. In particular, the latter provides the volume of the basins. In the cases for which the storage capacity (C) is absent, it is evaluated as:

$$C = \eta \cdot C_{water} \cdot H \quad (1)$$

where η is the turbine efficiency, assumed equal to 87% considering a reference value for a plant featuring a Pelton turbine. Such assumption is in many cases conservative, as it is applied also to plants where the more efficient Francis turbines are installed. The water capacity of the basin is expressed by C_{water}, while H represents the head (in m) from the dam to the turbine where the conversion into electricity occurs. In the cases for which the plant head is not explicitly provided, it is estimated from topological data.

Values at the plant level are then aggregated to have a regional detail, in order to comply with the resolution of the ESM (see Section 2.2). The final values are represented in Figure 1, and are used as input to the model to define the maximum capacity of each region.

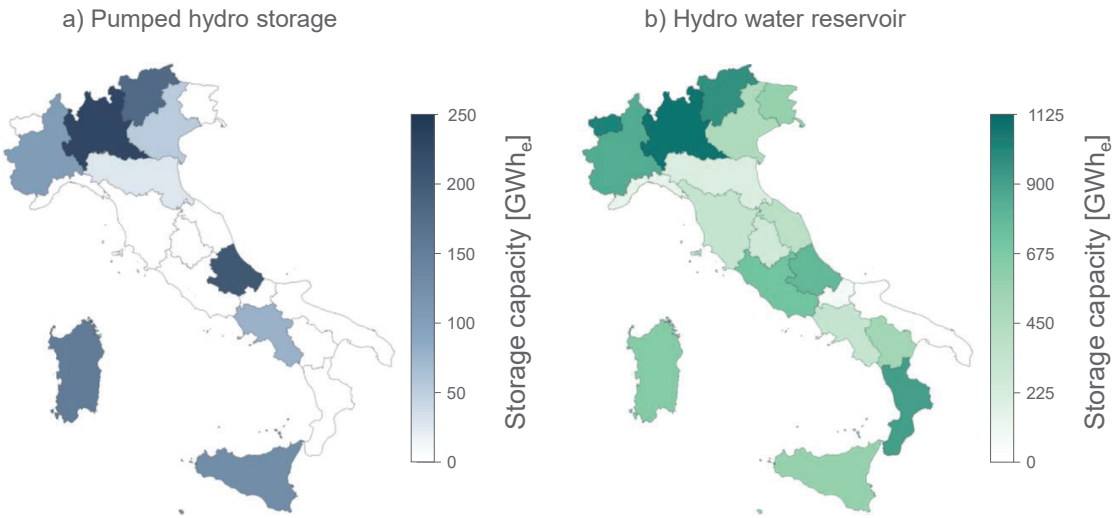

Figure 1. Energy storage capacity by region for (a) pumped hydro storage and (b) hydro water reservoir plants.

After having defined the capacities for each region, the water inflow is computed. This depends on the precipitations occurred in the watershed connected to each plant. However, detailed inflow data at a plant level are unavailable, and it is difficult to link a specific dam to the precipitation in the upstream portion of the watershed over a specific time period. Accordingly, the analysis considers the aggregate inflow by region.

The time series of the aggregate filling rate of HWR and PHS plants provided by ENTSO-E [7] is the starting point to derive the precipitation inflow. In particular, data represent the weekly-resolved estimation of the stored energy value (SEV) aggregated by bidding zone. The inflow time series is computed as:

$$Inflow_i = SEV_{i+1} - SEV_i + \sum_{j=1}^{168} (E_{HWR,j} + E_{PHS_{gen},j} - E_{PHS_{cons},j}) \quad (2)$$

where $E_{HWR,j}$, $E_{PHS_{gen},j}$, and $E_{PHS_{cons},j}$ are respectively the energy generated by reservoirs plants, the one generated by pumped storage plants, and the pumping consumption of pumped storage plants. Profiles of these quantities are available from ENTSO-E with an hourly resolution [10], so they are summed over each week of the year to be consistent with the SEV data. The *i* subscripts indicate the weeks in the year while the *j* ones represent the hours. To be consistent with the TSO inputs, a change in the ENTSO-E profiles is required. Indeed, since in the TSO data HWR are higher in terms of capacity, a compensation regarding the overall energy generated by them is needed not to underestimate the inflow. Consequently, the ENTSO-E profiles are scaled to match the overall generation by bidding zone provided by the TSO. The difference between the two data providers is due to different classification criteria regarding the type of hydropower plants. These are classified according to the time in which the overhead basin is filled by water stream. Specifically, the TSO sets as threshold between RoR and HWR a filling time of 2 hours, while ENTSO-E considers a value of 24 hours.

The resulting profiles represent what is assumed to be the charging or discharging of the bidding zone basins due to only the natural contributions (i.e., precipitations, evaporation, icing). As an example, Figure 2 shows the inflow profiles of two bidding zones (i.e., Centre-North and Sardinia). The inflow profiles clearly show that the distinct bidding zones feature seasonally different precipitation profiles. This is especially noticeable comparing northern and southern regions, where the basins are used as seasonal water storage to compensate the absence of rain during summer. Figure 2 also shows how, depending on the season, the inflow may also feature negative ones. These may result from evaporation and ice formation, or may be due

https://doi.org/10.52202/069564-0177

to maintenance of dams, which can require to empty the whole basin. Another reason may be the minimal vital flow that each river must provide and that, in the case it is regulated artificially, must be preserved through the spilling of water from reservoirs, especially in periods where no precipitations occur and the power plants are turned off. These data also show how in some regions (e.g., Sardinia) precipitations are extremely concentrated in time, highlighting importance of artificial basins for the river flow regulation.

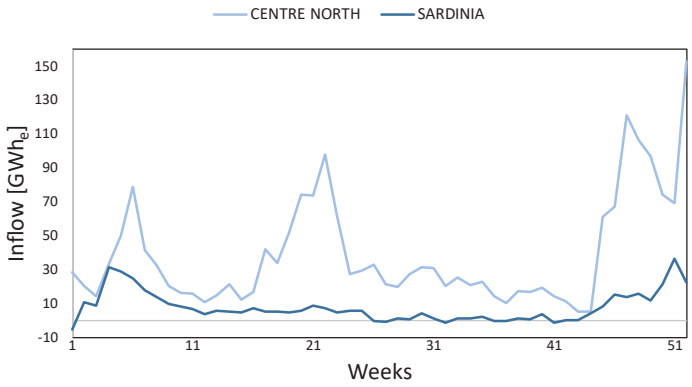

Figure 2. Inflow profiles of the Centre-North and Sardinia bidding zones.

The obtained inflow profiles must be distributed over the two different technologies (i.e., HWR and PHS) and over the regions that constitute each bidding zone. This is attained by dividing the inflow proportionally to the regional energy capacity of HWR and PHS plants (as previously derived). This is equivalent to assuming that plants with larger capacity benefit from a proportionately greater share of the bidding zone inflow.

2.2. Model description

The Italian energy system is modelled with the OMNI-ES model described in Ref. [5]. Considering a target year (2050 in this work), the model optimizes the national energy system by minimizing the total annual cost (including both capital and operational expenditures), covering all end-use sectors (residential and services, industry, road mobility, aviation, and navigation) and considering capacity expansion for all the included technologies adopting a brownfield approach. OMNI-ES is based on a multi-node formulation with a regional (NUTS-2) resolution and solves the energy balances on an hourly basis, adopting a perfect foresight approach. As

Figure **3** shows, the model encompasses a multiplicity of energy vectors (electricity, methane, hydrogen, liquid fuels – fossil, biogenic, or hydrogen-based) and the related transport networks, enabling the possibility to exploit the existing gas grid to deliver a blend of methane and hydrogen. In addition, OMNI-ES tracks the CO_2 flows considering carbon sources, sinks, and uses, in order to introduce a net-zero emission constraint.

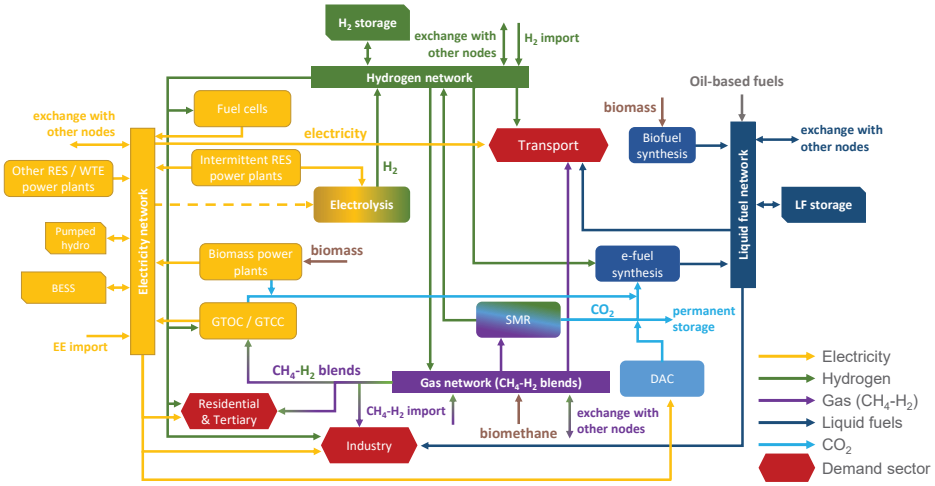

Figure 3. Schematised structure of the OMNI-ES model: nodal balances of energy vectors and CO_2 [5].

2.3. Scenario definition

This work applies the OMNI-ES model to investigate the role of hydroelectricity in a long-term scenario for Italy, considering 2050 as target year and enforcing the achievement of economy-wide carbon neutrality.

OMNI-ES requires as exogenous input the demand quantity and hourly profiles of each energy vector. Specifically, the analysis considers the evolution of all end-use sectors towards the adoption of decarbonized options. The resulting sectorial energy vector demand is summarized in Figure 4, considering the share by energy vector and the total annual demand by sector. The underlying assumptions are briefly presented in the remainder of this section, while a detailed discussion may be found in Ref. [5].

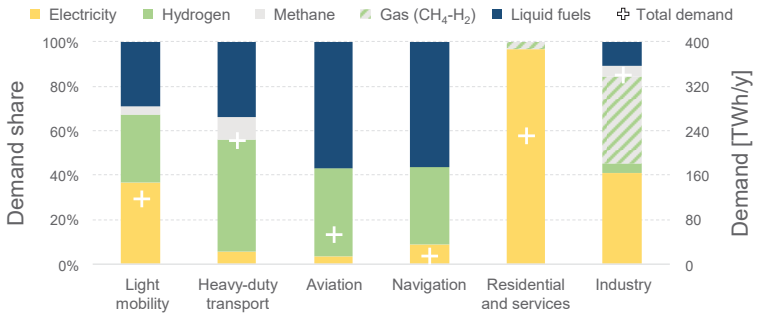

Figure 4. Demand of energy vectors by sector: shares on energy basis (left axis) and annual quantity (right axis).

The electric load encompasses the projection of the conventional consumers demand based on population and gross domestic product (GDP) growth and increased electrification in households, as assumed by the transmission system operators [11], and the additional demand from the electrification of building heating, transport, and industrial heat generation. The gas demand is assumed to be satisfied with a CH_4-H_2 blend with unconstrained hydrogen fraction, and takes into account the projected consumers demand as defined by the transmission system operator [11], a residual use of gas systems for heating of buildings, and high-temperature industrial heat generation. Pure hydrogen uses encompass applications in the transport sector and in industry, while liquid fuels are used in transport, considering the possibility to exploit carbon-neutral fuels in internal combustion engines, aviation, and navigation, and industry as chemical feedstocks.

In the heating sector, 75% of the thermal demand is assumed to be covered via electric heat pumps, 15% via district heating, 5% via gas absorption heat pumps, and 5% via biomass boilers. Cooling introduces an additional electricity demand, defined accounting for thermal comfort needs. The corresponding hourly-resolved profiles for each technology are determined following the methodology presented in Refs. [12–14].

Demand shares in transport are defined on the basis of recent long-term estimations for the sector [15,16]. The stock share assumptions for road transport (reported in Table 1) consider a massive presence of battery electric vehicles (BEVs) in light mobility, while hydrogen-powered fuel cell electric vehicles (FCEVs) and internal combustion engine vehicles (ICEVs) fed with liquid fuels (LF) are more relevant in heavy transport. The analysis also maintains the current reliance of part of road transport on pure CH_4, with use of either natural gas or biomethane. For aviation and navigation, demand shares are assigned considering the national consumption as reported in Figure 4, taking into account both passenger and freight transport.

Table 1. Road transport stock share assumptions.

Category	ICEV-LF	ICEV-CH_4	BEV	FCEV
Passenger cars	10%	-	75%	15%
Light-duty vehicles	20%	5%	50%	25%
Heavy-duty vehicles	20%	10%	10%	60%
Buses	15%	-	50%	35%

The industrial demand of energy vectors is built from historical consumptions [17], considering the adoption of decarbonized technologies. In particular, the analysis assumes the complete electrification of low-temperature (< 100 °C) process heat generation (excluding the systems already based on biomass, geothermal, and solar energy), while medium- and high-temperature (> 100 °C) heat generation based on oil derivatives and solid

https://doi.org/10.52202/069564-0177

fuels is considered to be converted to gas boilers fed by a CH_4-H_2 blend with hydrogen fraction up to 100%. Regarding the chemical industry, all fossil-based feedstocks are assumed to be converted to carbon-neutral options. This involves the replacement of natural gas in ammonia and methanol production with hydrogen, and the substitution of naphtha in high-value chemicals (HVC) and BTX (benzene, toluene, and xylenes) with carbon-neutral methanol [18]. Primary steelmaking is assumed to switch to Direct Reduction of Iron ore (DRI) and Electric Arc Furnaces (EAF), considering that, as DRI feed, half of the production relies on methane and half on hydrogen. The implementation of carbon capture and storage (CCS) is imposed for the methane-based production. Carbon capture and permanent sequestration is considered also in cement production.

The potentials for renewable energy sources are determined based on Ref. [5]. The solar photovoltaic potential is estimated to 405 GW_e, considering both rooftop- and ground-based plants, while the available wind speed and the geomorphological features of the territory limit the onshore wind potential to 224 GW_e. Considering areas with suitable wind intensity and seabed morphology for piled foundations [19], the offshore wind potential is set to 9.5 GW_e. For thermoelectric power generation, the analysis considers the revamping of combined-cycle gas turbines (CCGTs) and open-cycle gas turbines (OCGTs) with the installation of high-efficiency devices fuelled by CH_4-H_2 blend, as well as the phase out of oil- and coal-based plants. The maximum capacity of CCGTs and OCGTs is set 50% higher than current values (resulting in 83 GW_e for CCGTs and 5 GW_e for OCGTs), as revamping generally involves larger machinery. The biomass-based power generation potential is assumed equal to today's installed capacity (4 GW_e), as biomass availability is the main constraints for its exploitation. In accordance with national strategies, the operation of Waste-to-Energy (WtE) plants is kept unvaried (the installed capacity is currently 1 GW_e) [20]. As most available areas have already been exploited, only a slight increase of geothermal (+10%, reaching 1 GW_e) and run-of-river (+20%, reaching 7 GW_e) capacity is considered. For the same reason, the installed capacity of HWR and PHS is assumed unvaried (see Section 2 for the discussion on the current status of hydroelectric power generation).

Regarding domestic sources, the upper boundary for domestic gas production is set to the 2019 value, equal to 47 TWh_{LHV}/y, taking into account both onshore and offshore wells [21]. A biomass availability of 52 TWh_{LHV}/y is determined considering waste and residual solid biomass exclusively [22], while a biomethane production potential of 55 TWh_{LHV}/y is estimated considering the upgrading of biogas produced from livestock residues and biodegradable waste [22,23]. Finally, an annual storage capacity of 20 Mt_{CO2}/y is assumed as upper boundary for permanent CO_2 sequestration, corresponding to the lower boundary of the range indicated in the national long-term strategy [4].

2.4. Modelling of hydroelectric power generation

Based on the description provided, the aim is to analyze the impact of flexible hydropower operation on the national energy system in long-term scenarios with high levels of renewable energy penetration. To this end, two scenarios are investigated. The first does not enable hydropower flexibility of reservoir plants, assigning the operation of HWR plants based on historical generation profiles. The second scenario differs from the previous one in the way in which the reservoir plants are modelled. Here, the model selects the optimal plant operation, according to the equation:

$$Q_{HWR}^{r,t+1} = Q_{HWR}^{r,t} + \tilde{q}_{inflow,HWR}^{r,t} - \frac{q_{\mathrm{otp},HWR}^{r,t}}{\tilde{\eta}} \tag{3}$$

where, referring to the generic region r and time step t, $Q_{HWR}^{r,t}$ is the energy storage content of HWR plants, $\tilde{q}_{inflow,HWR}^{n,t}$ is the inflow as determined in Section 2.1, and $q_{\mathrm{otp},HWR}^{r,t}$ is the output power generation of HWR plants. Specifically, the inflow $\tilde{q}_{inflow,HWR}^{n,t}$ is an exogenous input data, while the storage content $Q_{HWR}^{r,t}$ and the power output $q_{\mathrm{otp},HWR}^{r,t}$ are model variables endogenously optimised.

The database developed in Section 2.1 provides the hourly profiles of natural inflow and the available storage capacity of HWR plants, which bounds the storage content in each region. To provide a realistic assessment, the initial level of the basins is imposed equal to the historical one at the first hour of the year. The level at the end of the year is instead imposed to be greater than or equal than the minimum value between the initial storage content and the historical end-of-year level. For this analysis the reference year, from which the historical data are derived, is the 2019. The choice is made to be consistent with the data used in Ref. [5], which considered 2019 as reference weather year. In addition, 2019 represents an average year for what concerns precipitations and basins filling levels. To conclude, the operation of pumped hydro storage plants is optimised in both scenarios, and run-of-river plants are modelled with assigned profiles equal to the historical ones, assuming a 20% capacity increase to account for new installations.

3. Results and discussion

Given the model description, the main assumptions, and the input data, the analysis compares the cost-optimal energy system configuration in a scenario with assigned HWR plant operation based on historical profiles (considered as reference) and in one with optimised flexible HWR operation.

Figure 5 shows the HWR duration curve comparison between the flexible and the assigned operation scenarios. The curve of the reference scenario features a smoother trend, as hydroelectricity has traditionally provided base load generation. When enabling flexible operation, HWR plants exhibit a peaking behavior, as the operating hours do not cover the whole year and the profile is shifted towards higher power values.

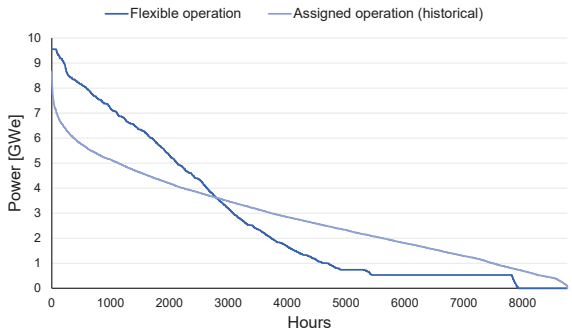

Figure 5. Duration curves of hydropower reservoir (HWR) plants in the flexible and in the reference scenarios.

Figure 6 shows the comparison of the storage energy value by bidding zone in both scenarios, following the geographical division of 2019. Specifically, the curve of the reference case is derived from historical data from ENTSO-E for the year 2019. In contrast, the flexible scenario aggregates results from individual regions across the bidding zones.

Figure 6. SEV comparison between the flexible scenario output and the 2019 profiles, for the aggregation of HWR and PHS basins in each bidding zone.

https://doi.org/10.52202/069564-0177

The model is allowed to vary between the maximum capacity of the basins, determined by the analysis illustrated in Section 2, and a minimum storage content, set equal to the historical minimum basin level. In some bidding zones (e.g., Sicily) the difference between the two lines is less marked, showing that using the assigned historical profiles does not represent a great difference, as HWR power generation is mostly driven by the availability of inflow. Instead, the curves are more distinct in bidding zones (e.g., Centre-South) resulting in a higher amount of energy stored during summer to be then discharged in autumn when photovoltaic generation is lower. Results reveal that the North bidding zone, which represents nearly 65% of the national value in terms of capacity, exhibits a trend similar to the historical one. However, it features a more pronounced seasonality, reaching differences of the energy stored during summer in the order of 1000 GWh_e.

These results show how hydroelectric basins operation can be assimilated to storage systems and that HWR detailed modelling can lead to a different optimal system configuration. In this regard, Table 2 shows the variation of the installed capacities of the most relevant technologies between the two scenarios. The introduction of HWR flexibility significantly impacts on the installation of battery energy storage systems (BESS), which feature a sensibly lower capacity in the flexible scenario. This is due to the possibility to exploit existing assets (i.e., hydroelectric plants) as storage systems, reducing the need for new installations that would represents an extra cost for the system. Indeed, the optimised use of HWR replaces BESS role in balancing short-term oscillations of renewable power generation. The availability of investment-free storage options enables a larger deployment of solar photovoltaic, which is the RES power generation technology with the lowest lower levelized cost of electricity, while the wind capacity undergoes a corresponding decrease. To avoid curtailment, the system relies on a larger hydrogen storage capacity, which is also used to compensate the greater seasonal unbalances that result from the additional PV installations. Gas turbine-based power generation capacity decreases by 22 %, as the flexible operation of HWR plants guarantees dispatchable electricity to assist the grid in hours where non-programmable sources are not available.

Table 2. Installation of main technologies.

Technologies	Reference scenario	Flexible scenario	Variation
Solar photovoltaic [GW_e]	311	338	+8%
Wind [GW_e]	130	127	-2%
Gas turbine-based power generation [GW_e]	17	15	-13%
Battery energy storage [GWh_e]	106	81	-24%
H_2 storage [GWh_{LHV}]	944	1212	+28%

Figure 7 focuses on the integration between PV and hydro reservoirs in the flexible operation scenario. The black line represents the cumulative duration curve of these two technologies, while stacked columns represent the share of HWR (in light blue) and photovoltaic (yellow) on the generated power in each hour. The figure shows a complementarity relation between solar PV and HWR, as the latter is used when solar radiation is scarce or not available. Indeed, the share of hydro reservoir generation starts to appear only at low power, increasing significantly in the right part of the chart.

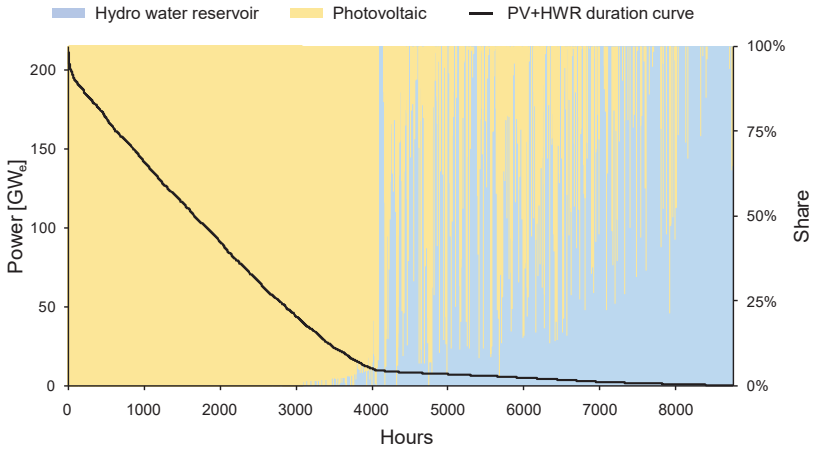

Figure 7. Cumulative PV and HWR duration curve (left axis) and hourly share on generated power (right axis).

Such behavior is also evident in Figure 8, which highlights that hydro reservoirs are adopted to compensate for the lack of PV generation during nighttime or low-solar-radiation days. The operation of the two systems features a strong daily pattern, with HWR covering the load in the early morning and late afternoon and PV taking over the central hours of the day. Consistent with the trend highlighted in Figure 5, HWR plants often operate at peak power. A certain degree of seasonal complementarity is also observed, as HWR generation in the central hours of the day intensifies in periods with low availability of solar radiation, such as the end of January, November, and December. Figure 8 also provides insights on the effect that the optimised management of hydroelectric systems has on reducing the need for BESS capacity, with the former compensating short-term renewable generation deficits.

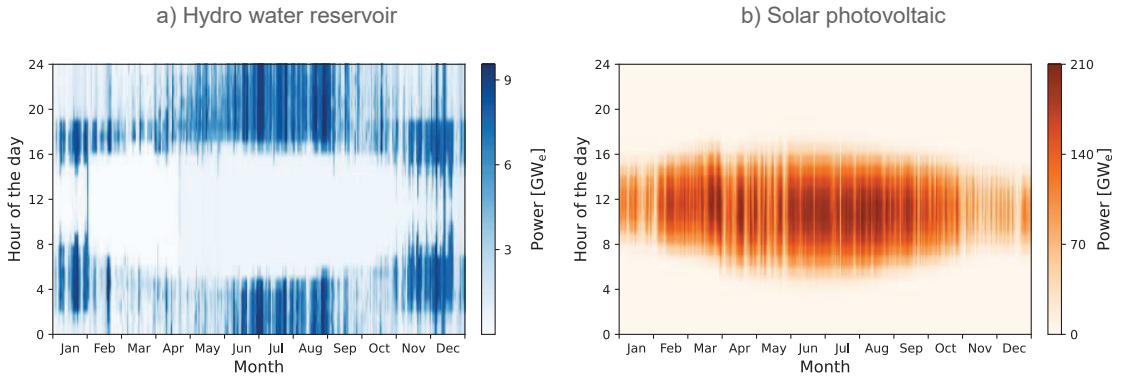

Figure 8. Hourly-resolved power generation profiles of hydro water reservoir (a) and solar photovoltaic (b).

4. Conclusions

The study presented in this work investigated the impact of hydropower flexibility on the Italian energy system, by introducing detailed hydropower data in a multi-node, multi-sector, and multi-vector energy system model. A comprehensive dataset of the programmable hydroelectric plants (pumped hydro and reservoirs) in Italy was created using open-source information. Compared to the available hydropower data sources, the developed dataset includes a complete list of plants, providing the nominal power and the energy storage capacity, which is typically unavailable in both national and European databases. Data have been aggregated to the regional level (NUTS-2) to compute the natural inflow profiles of HWR and PHS systems. The OMNI-ES energy system model was adopted to investigate the role of hydropower in economy-wide carbon-neutral scenarios. Adopting a perfect-foresight approach, the model application compared a flexible HWR operation scenario with optimised management of HWR plants, and an assigned operation scenario with HWR generation profiles based on historical data. The year 2019 was considered as reference for all the time series, while sensitivity analyses on the impact of the weather year are left to future assessments.

Results show that hydropower operation shifts from baseload to peak generation, thus acting as compensation of the intermittent generation of non-programmable sources. Accordingly, the system avoids the installation of additional flexibility elements, such as battery energy storage and gas turbine-based power generation, which feature a 24% and 13% capacity reduction compared to the assigned-operation scenario, respectively. Correspondingly, the optimised hydropower operation enables the deployment of additional solar photovoltaic capacity (+ 8%), leveraging its LCOE. Overall, the system is positively impacted by the possibility to perform both short-term and seasonal storage exploiting already existing assets, improving the integration of intermittent renewable sources in the energy system. Further developments of the work will involve the assessment of the impact of the reference climate year, considering different historical time series characterised by higher or lower precipitation. The effect of climate change will also be addressed, investigating the change of hydropower resources caused by global warming.

Nomenclature

Acronyms

BESS	Battery Energy Storage System
BEV	Battery Electric Vehicle
CCGT	Combined Cycle Gas Turbine
CCS	Carbon Capture and Storage
EAF	Electric Arc Furnaces

https://doi.org/10.52202/069564-0177

ESM Energy System Model
FCEV Fuel Cell Electric Vehicle
GDP Gross Domestic Production
HVC High Valuable Chemicals
HWR Hydro Water Reservoir
ICEV Internal Combustion Engine Vehicle
JRC Joint Research Centre
LF Liquid Fuels
OCGT Open Cycle Gas Turbine
PHS Pumped Hydro Storage
PV Photovoltaic
RES Renewable Energy Sources
RoR Run of River
SEV Storage Energy Value
TSO Transmission System Operator
WtE Waste to Energy

Symbols

C	Electric energy storage capacity
C_{water}	Water volume of hydropower basins
$E_{HWR,j}$	Energy generated by hydro water reservoir plants at hour j
$E_{PHS_{gen},j}$	Energy generated by pumped hydro storage plants at hour j
$E_{PHS_{cons},j}$	Energy consumed by pumped hydro storage plants at hour j
H	Head of hydropower plants
$Inflow_i$	Inflow to hydro water reservoir and pumped hydro storage plants in week i
SEV_i	Storage energy value of hydro water reservoir and pumped hydro storage plants in week i
$\tilde{q}^{r,t}_{inflow,HWR}$	Inflow to hydro water reservoir plants in region r and time step t
$Q^{r,t}_{HWR}$	Storage content of hydro water reservoir plants in region r and time step t
$q^{r,t}_{\mathrm{otp},HWR}$	Power output of hydro water reservoir plants in region r and time step t
η	Conversion efficiency of hydropower plants

References

[1] European Commission, COMMUNICATION FROM THE COMMISSION TO THE EUROPEAN PARLIAMENT, THE COUNCIL, THE EUROPEAN ECONOMIC AND SOCIAL COMMITTEE AND THE COMMITTEE OF THE REGIONS “Fit for 55”: delivering the EU’s 2030 Climate Target on the way to climate neutrality, 2021.

[2] European Commission, COMMUNICATION FROM THE COMMISSION TO THE EUROPEAN PARLIAMENT, THE EUROPEAN COUNCIL, THE COUNCIL, THE EUROPEAN ECONOMIC AND SOCIAL COMMITTEE AND THE COMMITTEE OF THE REGIONS REPowerEU: Joint European Action for more affordable, secure and sustainable energy, 2022.

[3] European Commission, Joint Research Centre, JRC Hydro-power database, (2019).

[4] Ministero dell’Ambiente e della Tutela del Territorio e del Mare, Ministero dello Sviluppo Economico, Ministero delle Infrastrutture e dei Trasporti, Ministero delle Politiche agricole Alimentari e Forestali, Strategia Italiana Di Lungo Termine Sulla Riduzione Delle Emissioni Dei Gas a Effetto Serra, 2021.

[5] P. Colbertaldo, F. Parolin, S. Campanari, A comprehensive multi-node multi-vector multi-sector modelling framework to investigate integrated energy systems and assess decarbonisation needs, Submitt. to Energy Convers. Manag. (2023).

[6] Terna, Terna: statistics 2019, (2019).

[7] ENTSO-E, Water Reservoirs and Hydro Storage Plants, (n.d.).

[8] F. Neumann, E. Zeyen, M. Victoria, T. Brown, Benefits of a Hydrogen Network in Europe, Preprint. (2022).

[9] Ministry of infrastructures and transport, Direzione generale per le dighe e le infrastrutture idriche, (n.d.).

[10] ENTSO-E, Actual Generation per Production Type - 2019, (n.d.).

[11] Terna, Snam Rete Gas, Relevant Scenario Report (Documento di Descrizione degli Scenari), 2022.
[12] M. Pozzi, G. Spirito, F. Fattori, A. Dénarié, J. Famiglietti, M. Motta, Synergies between buildings retrofit and district heating. The role of DH in a decarbonized scenario for the city of Milano, Energy Reports. 7 (2021) 449–457. https://doi.org/10.1016/j.egyr.2021.08.083.
[13] A. Dénarié, F. Fattori, G. Spirito, S. Macchi, V.F. Cirillo, M. Motta, U. Persson, Assessment of waste and renewable heat recovery in DH through GIS mapping: The national potential in Italy, Smart Energy. 1 (2021). https://doi.org/10.1016/j.segy.2021.100008.
[14] B. Dehghan B., T. Toppi, M. Aprile, M. Motta, Seasonal performance assessment of three alternative gas-driven absorption heat pump cycles, J. Build. Eng. 31 (2020) 101434. https://doi.org/10.1016/j.jobe.2020.101434.
[15] IEA, Net Zero by 2050, Paris, 2021.
[16] IRENA, Reaching Zero With Renewables, 2020.
[17] L. Mantzos, N. Matei, E. Mulholland, M. Rózsai, M. Tamba, T. Wiesenthal, The JRC Integrated Database of the European Energy System, European Commission, 2018.
[18] A.M. Bazzanella, F. Ausfelder, Low carbon energy and feedstock for the European chemical industry, 2017.
[19] P. Colbertaldo, S. Cerniauskas, T. Grube, M. Robinius, D. Stolten, S. Campanari, Clean mobility infrastructure and sector integration in long-term energy scenarios: The case of Italy, Renew. Sustain. Energy Rev. 133 (2020) 110086. https://doi.org/10.1016/j.rser.2020.110086.
[20] Decreto del Presidente del Consiglio dei Ministri 10 agosto 2016, Gazz. Uff. Della Repubb. Ital. (2016).
[21] Ministry of Economic Development, Data Book 2020, (2020).
[22] R. Pudelko, M. Borzecka-Walker, A. Faber, The feedstock potential assessment for EU-27 + Switzerland in NUTS-3. Deliverable D1.2 of the BioBoost project, 2013.
[23] Ministry of Health, Livestock Database, (2019).

 https://doi.org/10.52202/069564-0177